PROCEEDINGS OF SPIE

Wide-field two-photon microscopy with temporal focusing and HiLo background rejection

Elijah Y. S. Yew, Heejin Choi, Daekeun Kim, Peter T. C. So

SPIE.

Wide-field Two-photon Microscopy with Temporal Focusing and HiLo Background Rejection

Elijah Y. S. Yew[a], Heejin Choi[b], Daekeun Kim[b], Peter T. C. So[a,b,*]
[a]Singapore-MIT Alliance for Research and Technology, Singapore 117543; [b]Massachusetts Institute of Technology, Cambridge, MA02139
*ptso@mit.edu

ABSTRACT

Scanningless depth-resolved microscopy is achieved through spatial-temporal focusing and has been demonstrated previously. The advantage of this method is that a large area may be imaged without scanning resulting in higher throughput of the imaging system. Because it is a widefield technique, the optical sectioning effect is considerably poorer than with conventional spatial focusing two-photon microscopy. Here we propose wide-field two-photon microscopy based on spatio-temporal focusing and employing background rejection based on the HiLo microscope principle. We demonstrate the effects of applying HiLo microscopy to widefield temporally focused two-photon microscopy.

Keywords: Widefield two-photon, temporal focusing, structured illumination, background rejection

1. INTRODUCTION

The two-photon absorption process was first predicted by Dr. Göppert-Mayer in 1931 [1] and was developed by the groups of Dr. Sheppard and Dr. Webb into a powerful microscopic imaging technique for biology and medicine [2-4]. The photophysics differences between linear and nonlinear absorption is that in linear absorption, a single excitation photon at the required energy is absorbed and a single photon at the emission wavelength is emitted. In two-photon absorption two photons with half the energy (longer wavelength) are simultaneously absorbed and the emission photon of the same wavelength is emitted. In addition to fluorescence, second harmonic generation (SHG) may also be produced by optical interaction with molecules with non-centrosymmetric electron distribution with substantial polarizability. Non-symmetric responses of the electron distribution to the excitation field cause a re-radiation of the energy that contain the higher harmonics of the excitation field. Most of the following discussion will focus on fluorescence but is equally applicable to SHG imaging unless as noted. We will use the term multiphoton microscopy to cover both two-photon, SHG, and the corresponding higher order processes. Since nonlinear processes, such as two-photon absorption, require high laser peak power for efficient fluorophore excitation, pulses from a femtosecond laser are focused on a sample via a high numerical aperture objective. The fluorescence is collected by the objective and recorded by a photodetector. Since excitation occurs only at the focal point, raster scanning of the laser in 3D is required to map the fluorophore distribution in a specimen. This introduces a time difference between each point of the image and in cases where a long integration time is required, can result in an image that requires several seconds or even minutes to acquire.

Multiphoton microscopy has several advantages in 3D depth-resolved image acquisition. First, the quadratic dependence on photon flux results in inherent depth discrimination where over 80% of fluorescent signal is localized to within a 1 μm thick region. Second, photodamage and photobleaching is localized to this excitation volume. Third, the multiphoton excitation wavelength lies in the infrared region resulting in significantly lower tissue scattering and absorption and deeper imaging. Fourth, the wide separation of the excitation spectrum and the emission spectra allows more precise spectroscopic measurements.

Conventional fluorescence microscopy illuminates a sample using wide-field geometry resulting in rapid 2D images without depth resolution. In 3D optical microscopy such as conventional multiphoton microscopy, excitation light is focused to a diffraction-limited spot that results in optical sectioning but requires sequential raster scanning of the excitation volume to produce a 3D image. A consequence of raster scanning is that the image acquisition time becomes

slower as sample size or resolution increases. Finite fluorophore concentration and fluorescence saturation ultimately limits fluorescence photon generation rate even with very fast scanning mechanisms, such as acousto-optical deflectors. Therefore, the most effective way to improve imaging speed is to parallelize the excitation process. A highly successful approach utilizing this concept is the multifocal multiphoton microscopy (MMM) [5-8].

Here we present an alternative multiphoton imaging technique based on temporal focusing as described by Silberberg and co-workers and Xu and co-workers [9, 10]. In conventional focusing an optical pulse is focused in the spatial dimension while propagating along the axial direction. In a well corrected system, the temporal pulse width is ideally kept constant. The intensity at the focal spot reaches a maximum as a result of the spatial confinement. Nonlinear optical processes such as two-photon absorption are proportional to the square of the pulse peak power, resulting in optical sectioning. For a high numerical aperture (NA) objective, submicron lateral and axial resolution can be achieved. In contrast, during temporal focusing, the optical pulse again travels in the axial direction however the beam diameter does not change its spatial dimensions, which is unlike the conventional focusing. However, the instantaneous intensity will be maximized at the focal plane if the temporal width of the optical pulse can be manipulated spatially such that it is minimized at the focal plane. This approach allows wide-field imaging with depth discrimination because only at the focus will the intensity be high enough for two-photon absorption to occur.

The trick to generate temporal focusing is to control the temporal width of ultrafast pulses. The temporal width (τ) of an ultrafast pulse is related to its spectral bandwidth (Δv); the time-bandwidth product ($\tau \Delta v$) is a constant for transform-limited pulses. Therefore, the generation of broadened pulses can be accomplished by spectrally limiting their bandwidths. A very simple geometry to accomplish this task has been proposed by Silberberg and coworkers [11]. In the case of an aberration free lens, the optical path lengths from the back focal plane to the front focal plane are the same as in a 4-f system and are independent of the incidence angle of the ray relative to the optical axis. Therefore temporal focusing can be realized by introducing a dispersive element (diffraction grating) at the back focal plane of the tube lens. The effect of the grating is to break the input beam up into its spectral components which will eventually recombine at the focus of the objective. For a well corrected system, the pulse at the focus of the objective is the same as at the grating and the ultrafast pulse retains the narrow femtosecond pulse width with all spectral components overlapping. In the 4-f system, this path length matching property is true only between the back focal plane of tube lens and the front focal plane of the objective, but not anywhere else. As a result the pulse widths for the different spectral components are broad at all other planes outside the focal plane and the multiphoton excitation efficiency decreases. In this manner, such a widefield two-photon imaging system can also be used as a widefield micro-lithographic fabricator [12].

HiLo microscopy [13] is a two-step method of rejecting background signals using a principle similar to that of structured illumination [14, 15]. In HiLo microscopy two images with different illumination is needed to perform the background rejection. One image is captured with a 'uniform' illumination while the second image is captured using non-uniform illumination. The basis is that in the Fourier domain, the high frequency components are, by definition, in focus. This is the property of the optical transfer function of a widefield microscope where the high frequency components drop-off very rapidly with defocus. On the other hand the in-focus components of the image also consist of low frequency components which must be separated from the out of focus low frequency components. It is through the use of the projected grid at the focal plane that makes this possible. A mathematical explanation can be found in [16].

2. MATERIALS AND METHODS

A temporally focused, widefield two-photon microscope was setup as shown in Figure 1. The source was a Mai Tai HP operating at 780 nm with a pulse width of approximately 100 fs. The beam was expanded, collimated, and directed onto a blazed, 600 l/mm grating. The first-order diffracted beam from the grating was focused via a 250 mm focal length doublet at the back focal plane of the objective (Zeiss 40x, NA 1.2 water immersion). The HiLo microscope was incorporated by placing a mask at a pupil conjugate plane. In this manner the mask was projected onto the sample. The two-photon fluorescent signal was collected in an epi-detection manner and imaged through a Zeiss tube lens onto a GE680 ProSilica GigbitE CCD camera. The masks were basically grids of various periods (5 lp/mm and 10 lp/mm) were used. The HiLo images were processed offline with Matlab following the description given in [16].
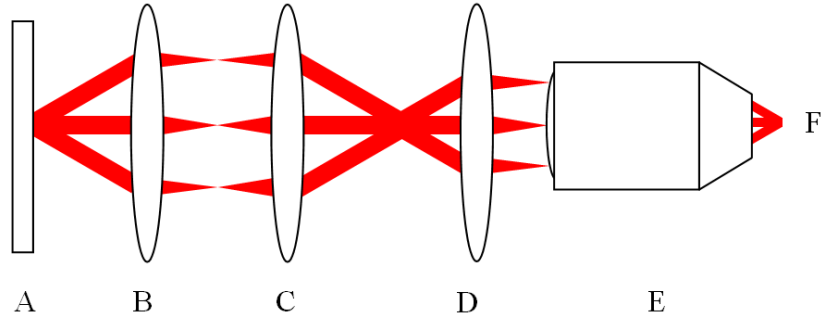
Figure 1. Schematic of a temporal focusing, widefield two-photon microscope with HiLo illumination. (A) Diffraction grating, (B) and (C) telescope arrangement, (D) tube lens, (E) objective, and (F) sample plane. The pupil plane between C and D allows for the introduction of a mask.

2.1 Theory of temporal focusing

The basis of temporal focusing is that a pulse from an ultrafast laser is not monochromatic but has a certain spectral bandwidth associated with the time-bandwidth product. In conventional microscopy that relies on nonlinear optical phenomenon (e.g. two-photon excitation), the beam is brought to a tight focus thereby increasing the intensity at the focus and also the probability of the two-photon excitation occurring. The spatial confinement therefore necessitates a beam scanning approach to generate a two-dimensional image. At the same time the temporal dimension of ultrafast pulses presents another possibility of increasing the intensity at the focus without compromising on the field-of-view.

For a transform limited pulse we can express the time-varying electric field before the grating as

$$A(x,t) = \exp\left[-\frac{t^2}{\tau^2}\right]\exp[i\omega_0 t]\exp\left[-\frac{x^2}{s_0^2}\right] \tag{1}$$

Where τ is the FWHM of the pulse width, ω_0 is the carrier frequency, and s_0 is the FWHM of the beam size. We have neglected the y dimension for simplicity although it is trivial to add it to the analysis. After the grating the electric field can be expressed as [17]:

$$E_2(x_2, y_2, \Delta\omega) = \exp\left[i\gamma\Delta\omega x_2\right]\exp\left[-\frac{\beta^2 x_2^2}{s_0^2}\right] \tag{2}$$

Where $\gamma = 2\pi m / d\omega_0 \cos[\theta_d]$, m is the diffraction order, d is the grating constant, θ_i, θ_d is the incident and diffraction angle respectively, and $\beta = \cos[\theta_i]/\cos[\theta_d]$. It is simple to obtain the electric field at the back focal plane of the objective, which is the Fourier transform of (2) i.e $E_3 = \mathsf{F}[E_2]$. At the focal plane the electric field can be found by expressing it as a Fourier transform of the field at the back focal plane of the objective giving:

$$E_5(x_5, y_5, \Delta\omega) = A(\Delta\omega^2)\frac{4f_1^2}{k^2}\exp\left[-\frac{\beta^2 M^2 x_5^2}{s_0^2} + i\gamma\Delta\omega M x_5\right] \tag{3}$$

3. RESULTS

A thin section (~ 16 microns) of prepared mouse kidney (Invitrogen, F24630) was imaged using the procedure as described in Materials and Methods. Figure 2 shows the uniformly illuminated image obtained with temporally focused

widefield two-photon microscopy. This image was common to both sets of non-uniformly illuminated images as shown later. The extent of the borders in the image represents a field of view of approximately 100 microns by 80 microns.
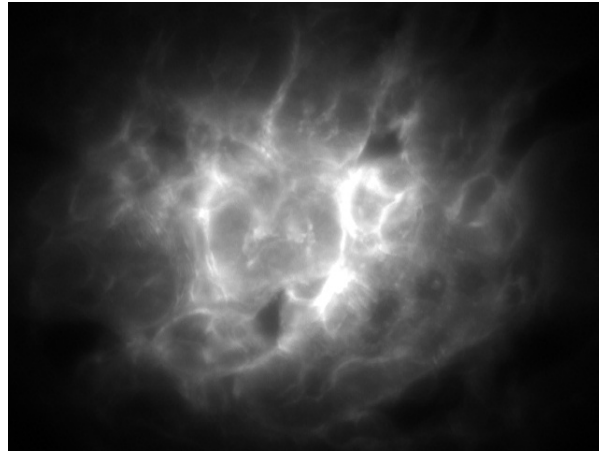

Figure 2. Temporally focused widefield two-photon image of a prepared mouse kidney on a glass slide.

Figure 3 illustrates the widefield two-photon images captured with two different types of non-uniform illumination. The figure on the left was taken with a 5 lp/mm Ronchi grating inserted as the mask. Given the specifications of our setup, this translated to approximately a grid period of 3.3 microns at the sample. The figure on the right shows the image with a 10 lp/mm Ronchi grating as the mask. This translated to a grid period of 1.65 microns at the sample. The integration time for the uniform image (Figure 2) was approximately 5 seconds while the integration time for the nonuniform illumination was 8 seconds and 12 seconds respectively for the grid of 5 lp/mm and 10 lp/mm respectively.
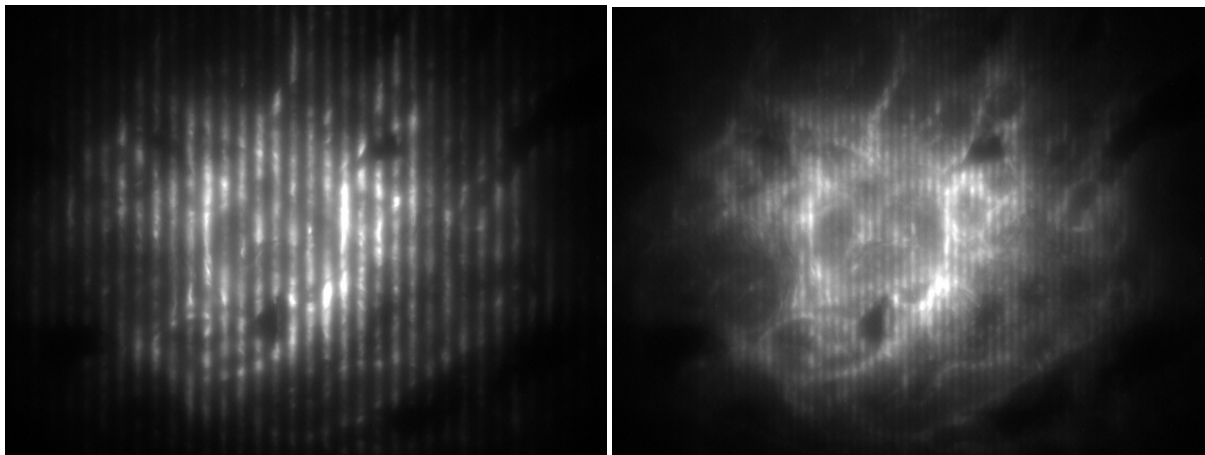

Figure 3. Temporally focused widefield with the projected grid pattern for (left) 5 lp/mm, and (right) 10 lp/mm.
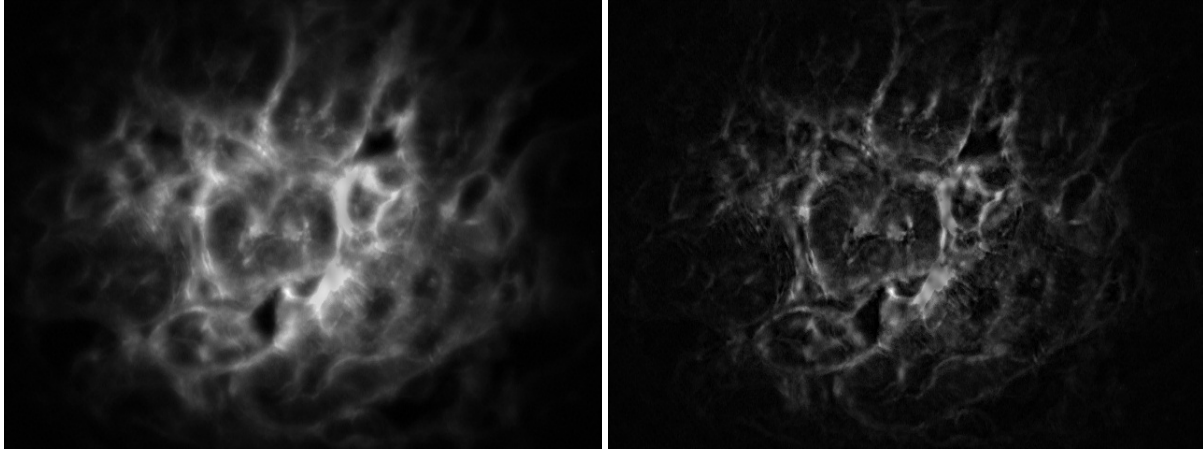
Figure 4. temporally focused widefield two-photon HiLo processed images for (left) 5 lp/mm, and (right) 10 lp/mm.

In Figure 4, we see the HiLo processed images. The figure on the left if the corresponding HiLo processed image for the 5 lp/mm grid projection and the figure on the right corresponds to the HiLo processed image for the 10 lp/mm.

4. DISCUSSION

It can be observed from Figure 2 that the uniformly illuminated image has a constant background that is due to the out of focus photons being detected at each pixel. This arises from the fact that the axial FWHM is poorer than that of a conventional spatial focusing two-photon microscope is because it is a widefield two-photon microscope. In a similar setup the measured FWHM in the axial direction was 2.27 microns [12]. It is clear that while we do have optical sectioning with a widefield temporally focused two-photon microscope the axial resolution is considerably poorer than that of a conventional spatial focusing two-photon microscope. The application of HiLo microscopy to our system results in a better optical sectioning without having to sacrifice field-of-view. In Figure 4, we see that effects of applying HiLo to our temporally focused two-photon microscope. It is clear from a comparison of Figure 4 and Figure 3 that it is possible to reject the out of focus photons and thereby improve the contrast of the image on the whole. At the same time high frequency components that were 'lost' because of the out of focus photons are visible as the grid spacing increases from 5 lp/mm to 10 lp/mm.

5. CONCLUSION

We have shown the feasibility of implementing HiLo microscopy in a two-photon microscope, specifically a widefield two-photon microscope based on temporal focusing. A widefield two-photon microscope is of particular interest because there is no need for beam scanning, which adds to the complexity and cost of the microscope. However the two-photon signal is imaged with a CCD camera, which makes it susceptible to image degradation by the out of focus photons. The overall effect of these photons is to lower the contrast and hence the imaging depth. HiLo microscopy has been shown to reject the out of focus photons and increase the image quality as well as enhance the in-focus objects of the image. It is thus useful for improving the image quality and extracting the in-focus information.

REFERENCES

[1]   M. Göppert-Mayer, "Über Elementarakte mit zwei Quantensprüngen," *Ann Phys (Leipzig),* vol. 5, pp. 273-94, 1931.
[2]   C. J. R. Sheppard*, et al.*, "The scanning harmonic optical microscope," in *IEEE/OSA Conference on Laser Engineering and Applications*, Washington, 1977, p. 100D.
[3]   J. N. Gannaway and C. J. R. Sheppard, "Second harmonic imaging in the scanning optical microscope," *Optics and Quantum electronics,* vol. 10, pp. 435-439, 1978.

[4]   W. Denk*, et al.*, "Two-photon laser scanning fluorescence microscopy," *Science,* vol. 248, pp. 73-6, 1990.

[5]   J. Bewersdorf*, et al.*, "Mulitfocal multiphoton microscopy," *Opt. Lett.,* vol. 23, pp. 655-657, 1998.

[6]   A. H. Buist*, et al.*, "Real time two-photon absorption microscopy using multipoint excitation," *J Microscopy,* vol. 192, pp. 217-26, 1998.

[7]   L. Sacconi*, et al.*, "Multiphoton multifocal microscopy exploiting a diffractive optical element," *Optics Letters,* vol. 28, pp. 1918-1920, Oct 15 2003.

[8]   T. Nielsen*, et al.*, "High efficiency beam splitter for multifocal multiphoton microscopy," *Journal of Microscopy-Oxford,* vol. 201, pp. 368-376, Mar 2001.

[9]   G. H. Zhu*, et al.*, "Simultaneous spatial and temporal focusing of femtosecond pulses," *Optics Express,* vol. 13, pp. 2153-2159, Mar 2005.

[10]   D. Oron*, et al.*, "Scanningless depth-resolved microscopy," *Optics Express,* vol. 13, pp. 1468-1476, Mar 2005.

[11]   D. Oron*, et al.*, "Single-pulse phase-contrast nonlinear Raman spectroscopy," *Phys Rev Lett,* vol. 89, p. 273001, Dec 30 2002.

[12]   D. Kim and P. T. C. So, "High-throughput three-dimensional lithographic microfabrication," *Opt Lett,* vol. 35, pp. 1602-4, May 15 2010.

[13]   D. Lim*, et al.*, "Wide-field fluorescence sectioning with hybrid speckle and uniform-illumination microscopy," *Opt Lett,* vol. 33, pp. 1819-21, Aug 15 2008.

[14]   M. G. Gustafsson, "Surpassing the lateral resolution limit by a factor of two using structured illumination microscopy," *J Microsc,* vol. 198, pp. 82-7, May 2000.

[15]   M. A. Neil*, et al.*, "Method of obtaining optical sectioning by using structured light in a conventional microscope," *Opt Lett,* vol. 22, pp. 1905-7, Dec 15 1997.

[16]   S. Santos*, et al.*, "Optically sectioned fluorescence endomicroscopy with hybrid-illumination imaging through a flexible fiber bundle," *Journal of Biomedical Optics,* vol. 14, 2009.

[17]   O. E. Martinez, "Grating and Prism Compressors in the Case of Finite Beam Size," *Journal of the Optical Society of America B-Optical Physics,* vol. 3, pp. 929-934, Jul 1986.